ON THE ARTIFICIAL COMPRESSION METHOD FOR SECOND-ORDER NONOSCILLATORY CENTRAL DIFFERENCE SCHEMES FOR SYSTEMS OF CONSERVATION LAWS

KNUT–ANDREAS LIE AND SEBASTIAN NOELLE

Abstract. The recently proposed high-order central difference schemes for conservation laws have a tendency of smearing linear discontinuities. In principle, Harten's artificial compression method (ACM) could be used to improve resolution. We analyse why this approach has not yet been used successfully and derive a more powerful version of the ACM based on a rigorous estimate of the total variation. Finally, we discuss the potential danger of overcompression and point out directions of future algorithmic development.

1. Introduction

The most successful and popular methods for computing solutions of hyperbolic systems of conservation laws are the upwind schemes originated by Godunov (1959) [1] and extended to second-order accuracy by van Leer (1979) [2]. A one-dimensional characteristic decomposition of the data makes it possible to update each wave-component of the solution in a stable and accurate manner. An alternative to the Godunov-type upwind schemes is the central difference scheme of Lax and Friedrichs (1954) [3], which was extended to second-order accuracy by Nessyahu and Tadmor in 1990 [4]. Central schemes resolve both smooth waves and shocks as sharply as comparable second-order upwind schemes. Since they apply no characteristic information or Riemann solvers, these schemes yield compact, efficient computer code and can in principle be used as black-box solvers. This attractive simplicity has lead to a widespread revival of the central schemes; see for example [5, 6] (third and fourth order), [7, 8] (two-dimensional Cartesian grids), [9, 10] (two-dimensional triangular grids), [11, 12] (non-staggered grids), and [13, 14, 15] (applications to relaxation systems, semiconductors, granular flows).

The main drawback of the Lax-Friedrichs-type central difference schemes in comparison with the Godunov-type upwind schemes is the smearing of linear discontinuities. Nessyahu and Tadmor [4] suggest two compression techniques to improve the resolution of linear waves:

The first version is a corrector step suggested by Harten which basically solves an inverse diffusion equation after every time-step. Since this step is applied to the full system, it may prevent the physically correct spreading of rarefaction waves. This may lead to entropy violating shocks.

The second technique - also inspired by Harten [16] - starts with a Roe-type characteristic decomposition of the numerical data [17]. A switch function should detect corners of linear discontinuities. Near these corners, a steeper (i.e., compressive) reconstruction is applied to the linear fields only. In the following, we will call this approach the artificial compression method (ACM). The advantage of ACM over the inverse diffusion technique described above is that it avoids entropy violating shocks, which can only occur in the nonlinear fields.

Date: Submitted for publication to SIAM Journal on Scientific Computing. July 27, 2001.

Surprisingly, Nessyahu and Tadmor do not show numerical experiments with this second version of ACM in their paper [4]. This gap is the starting point of the present note.

In the following we will analyse the ACM for the linear scalar advection equation and show that in this context it is equivalent to a standard second-order scheme with a certain limiter function. This limiter is a special case of a one-parameter family of limiters. Another member of this family is van Leer's limiter function, which is **not** compressive. We show that Harten's version of ACM as described in [4] is even **less** compressive than van Leer's limiter.

A sharp estimate of the total variation (TV) allows us to derive the range of TVD (TV decreasing) limiters, among them limiters that are much more compressive than van Leer's. Numerical experiments confirm the impressive power of these limiters.

Unfortunately, this is not the end of the story: the power of the ACM is also its potential failure. Smooth linear waves may be overcompressed into piecewise linear ones with sharp corners, or even into step functions. Harten's switch function, designed to monitor the smoothness of the solution and the admissible amount of artificial compression, fails to distinguish between corners of a step, where compression should be applied, and smooth extrema, where it should not be used. We conclude our note by pointing out the narrow ground for future algorithmic improvement.

In work parallel to this, Kurganov and Petrova [18] have developed another variant of Harten's ACM for the nonstaggered central scheme [12] and also demonstrated its potential to sharpen linear waves.

2. TVD analysis for central difference schemes

To make our point as transparent as possible, we assume that the standard characteristic decomposition has already been carried out. Hence we restrict our attention to the one-dimensional, linear, scalar advection equation

$$u_t + f(u)_x = 0, \quad f(u) = au. \tag{1}$$

The NT (Nessyahu-Tadmor) scheme can be written in the general conservative staggered form

$$u_{i+\frac{1}{2}}^{n+1} = \frac{1}{2}(u_i^n + u_{i+1}^n) - \lambda(g_{i+1}^n - g_i^n) \tag{2}$$

with numerical flux

$$g_i^n = f(u_i^{n+\frac{1}{2}}) + \frac{1}{8\lambda}u_i'. \tag{3}$$

Here $\lambda = \frac{\Delta t}{\Delta x}$ and $u_i^{n+\frac{1}{2}}$ is an intermediate value obtained by the predictor step

$$u_i^{n+\frac{1}{2}} = u_i^n - \frac{\lambda}{2}f_i'. \tag{4}$$

The values u_i' and f_i' are numerical approximations of the derivatives $\Delta x u_x$ and $\Delta x f(u)_x$ and will be specified below.

The following Lemma of Nessyahu and Tadmor carries over Harten's TVD result [16, Lemma 2.2] to the staggered schemes:

Lemma 1. *The scheme* (2) *is TVD if*

$$\lambda\frac{|g_{i+1} - g_i|}{|u_{i+1} - u_i|} < \frac{1}{2}. \tag{5}$$

For the proof, see [4, Lemma 3.1]. Now let

$$\nu := \lambda a \tag{6}$$

be the Courant number. Throughout the following, we always assume that the time-step satisfies the Courant–Friedrichs–Lewy (CFL) condition

$$|\nu| < \frac{1}{2}. \tag{7}$$

Note that (5) is the discrete analog of (7). Now we use the linearity of the flux function to simplify the scheme:

$$u_i^{n+\frac{1}{2}} = u_i^n - \frac{\nu}{2} u_i' \tag{8}$$

and

$$\lambda g_i^n = \nu u_i^n + \frac{1-4\nu^2}{8} u_i'. \tag{9}$$

Therefore,

$$\lambda(g_{i+1}^n - g_i^n) = \left(\nu + \frac{1-4\nu^2}{8}\frac{u_{i+1}' - u_i'}{u_{i+1} - u_i}\right)(u_{i+1} - u_i). \tag{10}$$

Lemma 1 implies that the scheme (2) will be TVD provided that

$$\left|\nu + \frac{1-4\nu^2}{8}\frac{u_{i+1}' - u_i'}{u_{i+1} - u_i}\right| \le \frac{1}{2}. \tag{11}$$

In the following we consider reconstructions of the form

$$u_i' = \phi\left(\frac{u_{i+1} - u_i}{u_i - u_{i-1}}\right)(u_i - u_{i-1}). \tag{12}$$

The Lipschitz-continuous function ϕ is called the limiter; see Sweby (1984) [19]. We require that these limiters satisfy the symmetry condition

$$\phi(r) = r\phi(\frac{1}{r}). \tag{13}$$

Therefore, we can also express the numerical derivative u_i' in terms of the right-sided differences,

$$u_i' = \phi\left(\frac{u_i - u_{i-1}}{u_{i+1} - u_i}\right)(u_{i+1} - u_i). \tag{14}$$

We have the following consequence of condition (11):

Lemma 2. *The scheme* (2), (9), (12) *is TVD if*

$$\phi(r) = 0 \quad \text{for} \quad r < 0 \tag{15}$$

and

$$0 \le \phi(r) \le \frac{4}{1+2|\nu|}\min(r, 1) \quad \text{for} \quad r \ge 0. \tag{16}$$

The elementary proof is analogous to Sweby's derivation of the sufficient TVD-condition [19, eq. (3.12)]. We omit the details.

If we set $4/(1+2|\nu|)$ to its minimal value of 2 (obtained for $|\nu| = 0.5$), then these conditions coincide with the TVD-constraints of Sweby for non-staggered schemes. Recall that these limiters lead to second-order accurate schemes away from extrema if

$$\phi(1) = 1. \tag{17}$$

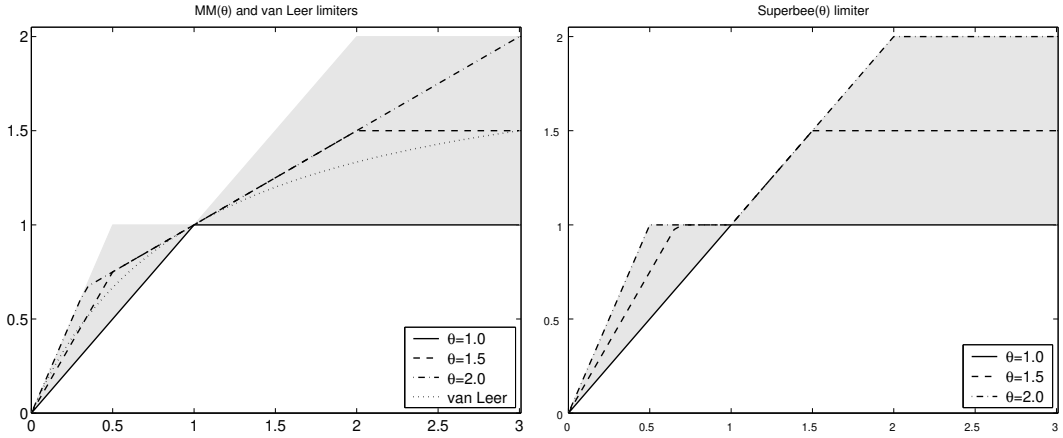

FIGURE 1. Sketch of MM, VL and SB limiters.

To this, we would like to add the stricter accuracy condition

$$(\phi(r) - 1)(\phi(r) - r) \leq 0, \tag{18}$$

which is equivalent to requesting that the resulting slope will be a convex combination of the left-sided and right-sided difference quotients. Of course, (18) implies (17). Examples of second-order accurate TVD limiters are van Leer's limiter (VL),

$$\phi^{VL}(r) := \frac{r + |r|}{1 + |r|},$$

the family of MinMod limiters (MM_θ)

$$\phi_\theta^{MM}(r) := \max\{0, \min\{\theta r, \frac{1+r}{2}, \theta\}\},$$

for $1 \leq \theta \leq 4/(1 + 2|\nu|)$, and the family of Superbee limiters (SB_θ)

$$\phi_\theta^{SB}(r) := \max\{0, \min\{\theta r, 1\}, \min\{r, \theta\}\},$$

again for $1 \leq \theta \leq 4/(1 + 2|\nu|)$. See Figure 1.

In Figure 2 we show computations of a periodic step function and a sine wave using various limiters and CFL-number $\nu = 0.2$. Note that while it may be desirable to choose a larger CFL number, say 0.4, for the problem at hand, the lower CFL number here is motivated from gas dynamics. There the time-step is calculated using the fastest wave speed, which occurs in the nonlinear acoustic wave. If the Mach number is around unity (i.e., $|v| \approx c$), then the speed $|v|$ of the linear field is only half that of the faster nonlinear speed $|v| + c$, so the effective CFL number for the linear field will be only one half that of the overall algorithm. We compute 20 temporal periods using 160 grid points. This corresponds to 16.000 time-steps.

Clearly, all computations are total-variation stable. For the MM ($= \mathrm{MM}_1$) and VL limiters the numerical results are dominated by dissipation. After 20 periods, the step resembles a steep, but smooth wave. As time proceeds, the solution will become more and more smeared. Compare the results for the SB ($= \mathrm{SB}_2$) limiter. Here the step is resolved within a few mesh-points, and it does not spread with time. On the other hand, the smooth sine wave has developed two corners near the extrema for the SB limiters. Clearly, the challenge lies in designing reconstructions that work well both for smooth and discontinuous solutions.

3. Harten's Artifical Compression Method (ACM)

This question was treated in 1983 by Harten [16]. In his artificial compression method (ACM) he starts the reconstruction with the standard MinMod (MM) limiter. To this, he adds an additional contribution near the corners of a jump-discontinuity, making the limiter compressive. The core of the ACM is a switch-function that quantifies how much compression may be used. The resulting reconstruction reads

$$u_i' = MM(u_{i+1}-u_i, u_i-u_{i-1}) + \theta_i MM(\sigma_{i+\frac{1}{2}}(u_{i+1}-u_i), \sigma_{i-\frac{1}{2}}(u_i-u_{i-1})) \tag{19}$$

where $MM(a,b) := \phi_1^{MM}(\frac{a}{b})\cdot b$. The switch θ_i is given by

$$\theta_i = \frac{|u_{i+1}-2u_i+u_{i-1}|}{|u_{i+1}-u_i|+|u_i-u_{i-1}|}. \tag{20}$$

Remark 3. *Note that the addition of artificial compression does not destroy the formal second-order accuracy of the underlying TVD-scheme, because θ_i is $O(\Delta x)$ in smooth parts of the solution away from the extrema. Near extrema $\theta_i = O(1)$, but at extrema TVD schemes can only be first-order accurate anyway.*

The parameters $\sigma_{i+\frac{1}{2}}$ are given as

$$\sigma_{i+\frac{1}{2}} = \sigma(\nu_{i+\frac{1}{2}}), \tag{21}$$

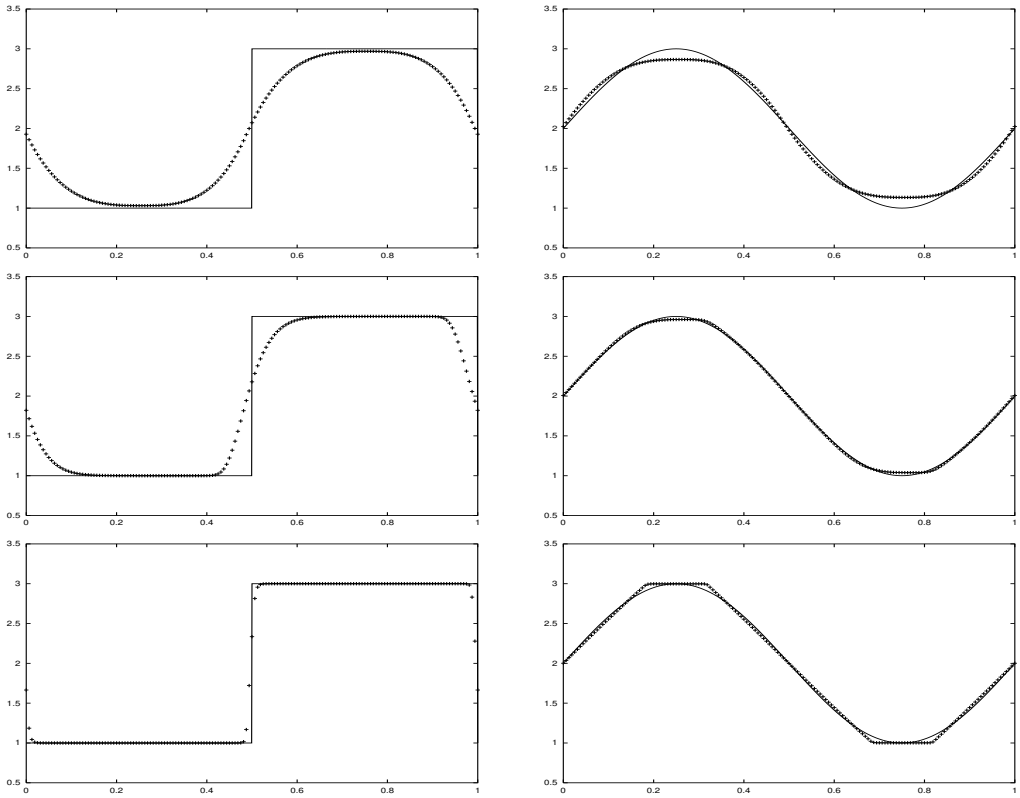

Figure 2. Computations of a periodic step (left column) and a sine wave (right column) using various limiters. 160 points, 20 periods (16.000 time-steps), CFL = 0.2. From top to bottom: MM_1, VL, SB_2.

where $\nu_{i+\frac{1}{2}}$ is the local CFL number. In the linear advection case considered in this section, $\nu_{i+\frac{1}{2}} \equiv \nu$. In order to obtain a TVD bound for his scheme, Harten [16, eq.(5.1)] requests that

$$0 \le \sigma(\nu) \le 1 - |\nu| - \frac{1}{2}(Q(\nu) - |\nu|^2). \tag{22}$$

Here $Q(\nu)$ is the numerical viscosity of the basic numerical function used. Typical values are $Q(\nu) = |\nu|$ or $Q(\nu) = |\nu|^2$, the latter being the viscosity of the Lax–Wendroff flux. In any case, $Q(\nu) \ge |\nu|^2$.

Harten suggests to use

$$\sigma(\nu) = \frac{1}{2}(1 - Q(\nu)). \tag{23}$$

In particular, this gives

$$\sigma(\nu) < \frac{1}{2} \quad \text{for} \quad \nu \neq 0. \tag{24}$$

We now use Lemma 2 to derive a less restrictive TVD condition on $\sigma(\nu)$. Let

$$r_i = \frac{u_i - u_{i-1}}{u_{i+1} - u_i}.$$

From this and (20) we obtain

$$\theta_i = \frac{|1 - r_i|}{1 + |r_i|}. \tag{25}$$

Due to the symmetry assumption (13), we may restrict the discussion to the case $0 \le r \le 1$, so $\phi_1^{MM}(r) \equiv r$. Therefore, the reconstruction (19) becomes

$$u_i' = \phi_\sigma^{ACM}(r_i)(u_{i+1} - u_i) \tag{26}$$

with

$$\phi_\sigma^{ACM}(r) = r + \frac{1 - r}{1 + r}\sigma(\nu)r. \tag{27}$$

According to Lemma 2 this reconstruction will be TVD if

$$0 \le \phi_\sigma^{ACM}(r) \le \frac{4r}{1 + 2|\nu|}. \tag{28}$$

In terms of the function $\sigma(\nu)$, this reads

$$0 \le \sigma(\nu) \le \frac{1 + r}{1 - r}\left(\frac{4}{1 + 2|\nu|} - 1\right). \tag{29}$$

Taking the minimum of the right-hand-side of this inequality over $r \in [0, 1]$ we obtain the following sufficient condition:

Lemma 4. *The reconstruction* (26) *and* (27) *is TVD provided that*

$$0 \le \sigma(\nu) \le \frac{4}{1 + 2|\nu|} - 1 =: \sigma_{max}(\nu). \tag{30}$$

Note that

$$1 \le \sigma_{max}(\nu) < 3 \quad \text{for} \quad 0 < \nu < \frac{1}{2} \tag{31}$$

which is two to six times as much as the value of $\sigma(\nu) < \frac{1}{2}$ admitted by (24)! We will use this freedom to derive a scheme that is more compressive than the one suggested by Nessyahu and Tadmor. Suppose first that we would like to construct a TVD-limiter that is independent of

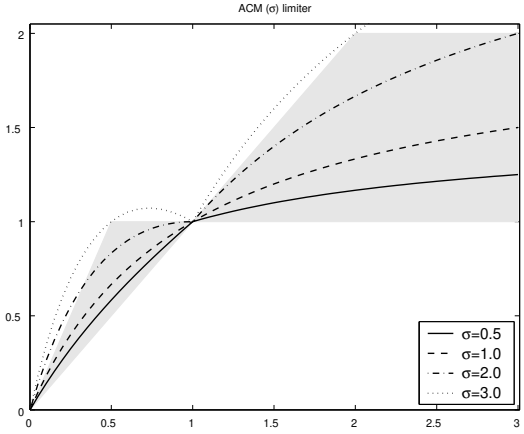

FIGURE 3. Sketch of the family of ACM limiters for $\sigma = 0.5, 1.0, 2.0, 3.0$.

the local value of ν. In this case we minimise the right-hand-side of (30) over $\nu \in [0, \frac{1}{2}]$ and obtain

$$\sigma(\nu) \equiv 1.$$

Remark 5. *It can easily be checked that*

$$\phi^{ACM}_{\sigma=1}(r) = r + \frac{1-r}{1+r}r = \frac{2r}{1+r} = \phi^{VL}(r)$$

so we recover van Leer's limiter function, which leads to a rather dissipative numerical scheme. This may explain why no numerical results using ACM where shown in [4]*: they would have been even more dissipative than those for van Leer's limiter in Figure 2.*

Therefore, if we want to have any chance of resolving a discontinuous solution within a few mesh points in the large time range, we have to go to higher values of σ. For

$$1 \le \sigma \le \sigma_{max}$$

the family of ACM- limiters may be rewritten as

$$\phi^{ACM}_{\sigma}(r) = \max\left\{0, \frac{r(\sigma+1) - r^2(\sigma-1)}{r+1}, \frac{r(\sigma+1) - (\sigma-1)}{r+1}\right\}. \tag{32}$$

For $\sigma \le 2$, $\phi^{ACM}_{\sigma}(r)$ is still monotone as a function of r, but it becomes non-monotone as σ takes values higher than 2; see Figure 3.

In Figure 4, we show numerical results for our family of ACM limiters. Clearly, we see the compressive effect as σ increases from the van Leer value of unity to larger values. Note that for $\nu = 0.2$, $\sigma_{max} = 1.867 < 2$, so the limiter is still monotone as a function of r. In Figure 5 we show the result for $\nu = 0.05$ and $\sigma = \sigma_{max} = 2.6364$. With these parameters, the sine wave is compressed into a step function.

4. Classification of TVD limiter functions

Based on the numerical evidence accumulated so far, we would like to suggest the following definition:

Definition 6. *Suppose that the limiter function $\phi(r)$ is Lipschitz continuous, satisfies the symmetry condition* (13)*, the accuracy condition* (17) *and the TVD conditions* (15) *and* (16)*. Then we call ϕ:*

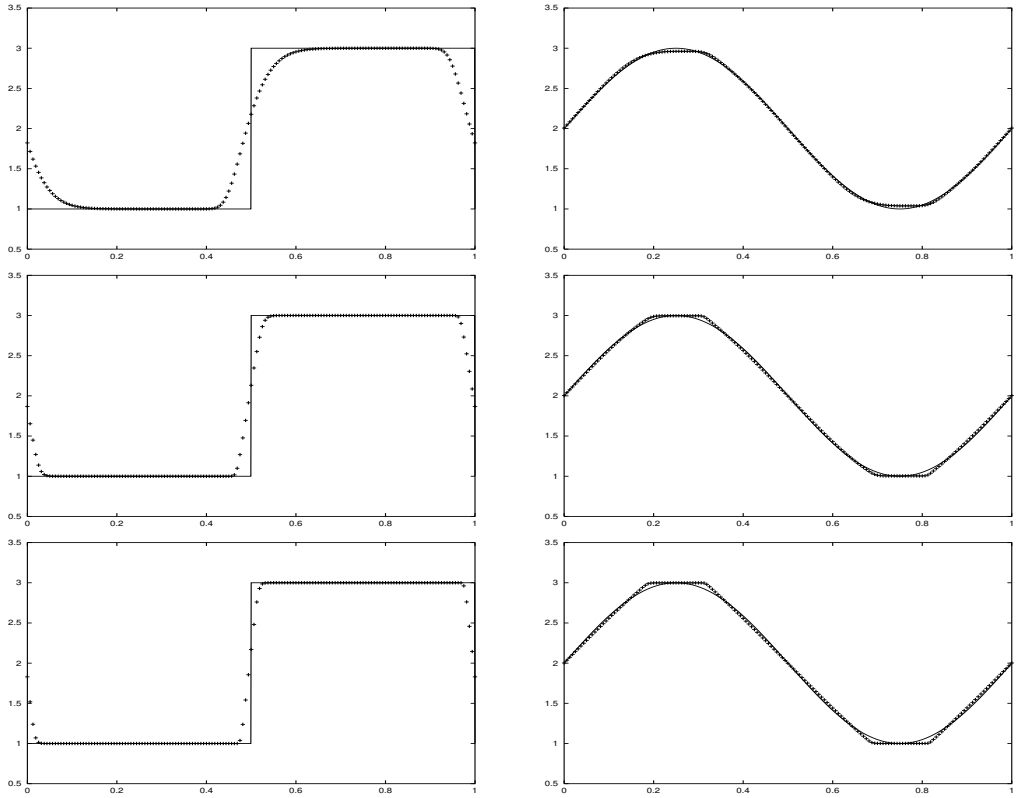

FIGURE 4. Same as previous figures, but using Harten's ACM limiter with $\nu = 0.2$ and $\sigma = 1, 1.5, \sigma_{max} = 1.867$.

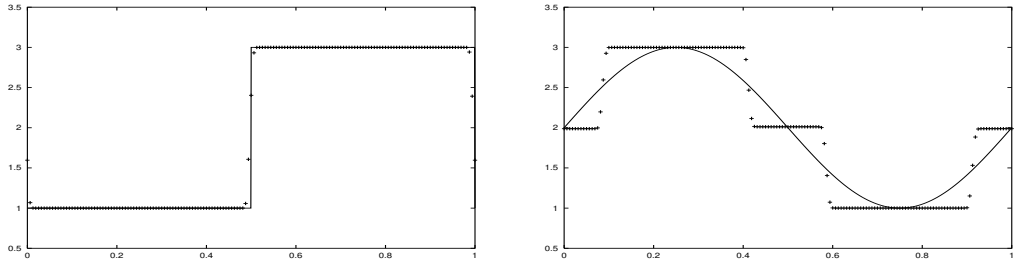

FIGURE 5. Same as previous figures, but using Harten's ACM limiter with $\nu = 0.05$ and $\sigma = \sigma_{max} = 2.636$.

(i) ***strictly dissipative*** *if* $\lim_{r\to 1-} \phi'(r) > \frac{1}{2}$,

(ii) ***dissipative*** *if* $\lim_{r\to 1-} \phi'(r) \geq \frac{1}{2}$,

(iii) ***well-balanced*** *if* $\lim_{r\to 1-} \phi'(r) = \frac{1}{2}$,

(iv) ***compressive*** *if* $\lim_{r\to 1-} \phi'(r) < \frac{1}{2}$,

(v) ***overcompressive*** *if* $\lim_{r\to 1-} \phi'(r) < 0$,

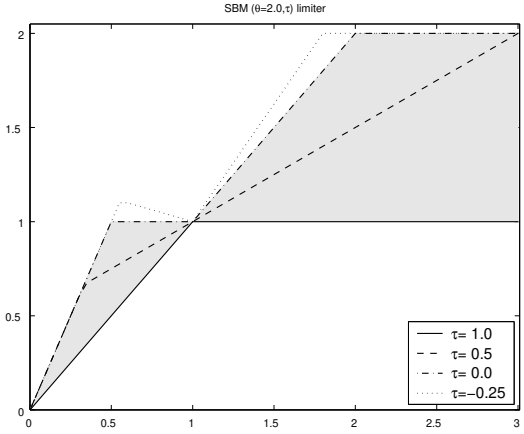

FIGURE 6. Sketch of the family of SBM limiters for $\theta = 2.0$ and $\tau = 1.0, 0.5, 0.0, -0.25$.

Note that the symmetry condition (13) implies that

$$\phi'(r) = \phi\left(\frac{1}{r}\right) - \frac{1}{r}\phi'\left(\frac{1}{r}\right),$$

so

$$\lim_{r\to 1-} \phi'(r) = 1 - \lim_{r\to 1+} \phi'(r). \tag{33}$$

For a well-balanced limiter left- and right-sided derivatives coincide at $r = 1$, and

$$\phi'(1) = \frac{1}{2} \tag{34}$$

The idea of our definition is to call a limiter compressive if away from extrema of the solution, the resulting reconstruction is steeper than the centred difference quotient.

Remark 7. *According to our definition,*

(i) *the family of Superbee limiters is compressive for $\theta > 1$,*
(ii) *van Leer's limiter as well as the family of MinMod limiters for $\theta > 1$ are well-balanced,*
(iii) *the MinMod1 limiter is strictly dissipative.*

Note also that overcompressive limiters satisfy the accuracy requirement (17) by definition, but violate the stricter accuracy requirement (18).

Even more important in our context is the following

Remark 8. *The limiter that results from Nessyahu and Tadmor's adaptation of Harten's ACM is not compressive, but* ***strictly dissipative*** *according to our definition.*

As a final remark, we would like to introduce a modified family of Superbee limiters that is directly based on Definition 6:

$$\phi^{SBM}_{\theta,\tau}(r) := \max\{0, \min\{r\theta, 1 + \tau(r-1), \theta\}, \min\{1 + (1-\tau)(r-1), \theta\}\} \tag{35}$$

Note that

$$\tau = \lim_{r\to 1-} \phi'(r)$$

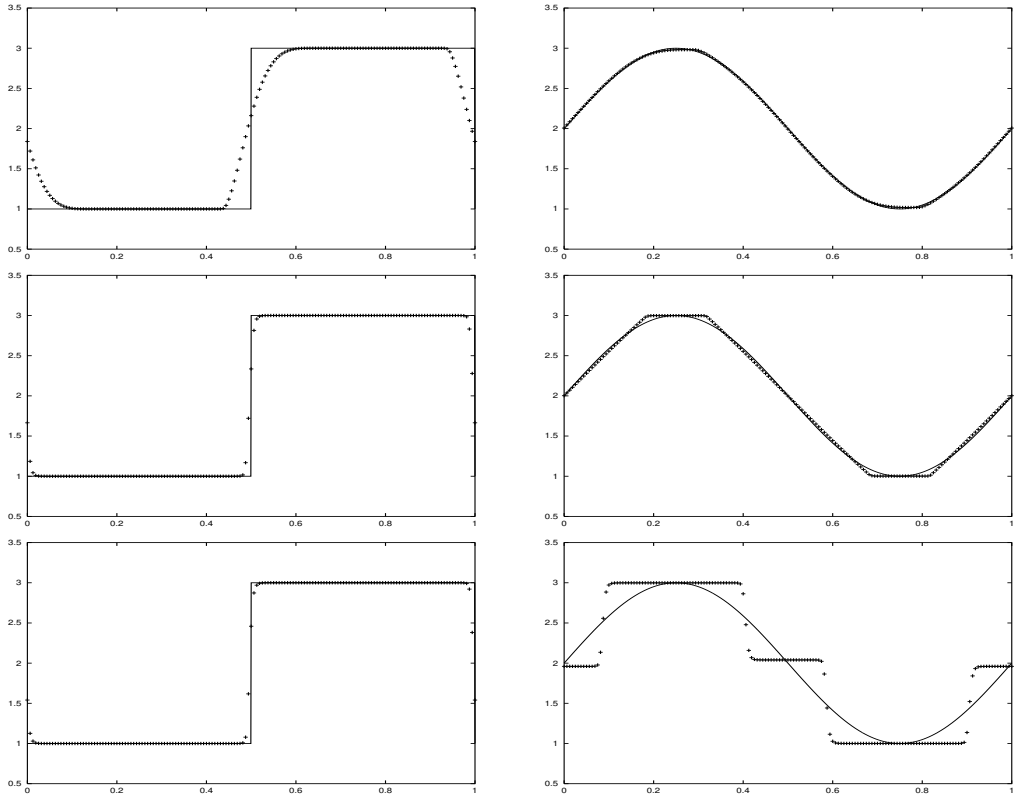

FIGURE 7. Same as previous figure, but using SBM limiter with $\theta = 2.0$ and $\tau = 0.5, 0.0, -0.25$ (from top to bottom).

and that

$$\begin{aligned} \phi^{SBM}_{\theta,1} &= \phi^{MM}_{1} \\ \phi^{SBM}_{\theta,\frac{1}{2}} &= \phi^{MM}_{\theta} \\ \phi^{SBM}_{\theta,0} &= \phi^{SB}_{\theta} \end{aligned}$$

The new limiter becomes overcompressive for negative values of τ. Figure 6 contains a sketch of this limiter for $\theta = 2$ and $\tau = 1.0, 0.5, 0.0, -0.25$.

In Figure 7 we display numerical results for $\theta = 2$ and $\tau = 0.5, 0.25, -0.25$. The effects of dissipation (for $\tau = 0.5$, MM_2 case), compression ($\tau = 0.0$, SB_2 case) and overcompression ($\tau = -0.25$) are clearly distinguishable: for smooth data the compressive SB limiter lead to kinks, i.e., jumps in the first derivative of the numerical solution, while the overcompressive limiter leads to jumps in the solution itself.

5. Compressible gas dynamics

To demonstrate the power of the ACM approach, we study an example from one-dimensional gas dynamics. The example describes a moving Mach 3 shock that interacts with a turbulent flow represented by a sine wave in the density. The initial configuration is as follows

$$(\rho, u, p)(x, 0) = \begin{cases} (3.857143, 2.629369, 10.33333), & x < -4 \\ (1 + 0.2 \sin 5x, 0, 1.0), & x \geq -4. \end{cases} \tag{36}$$

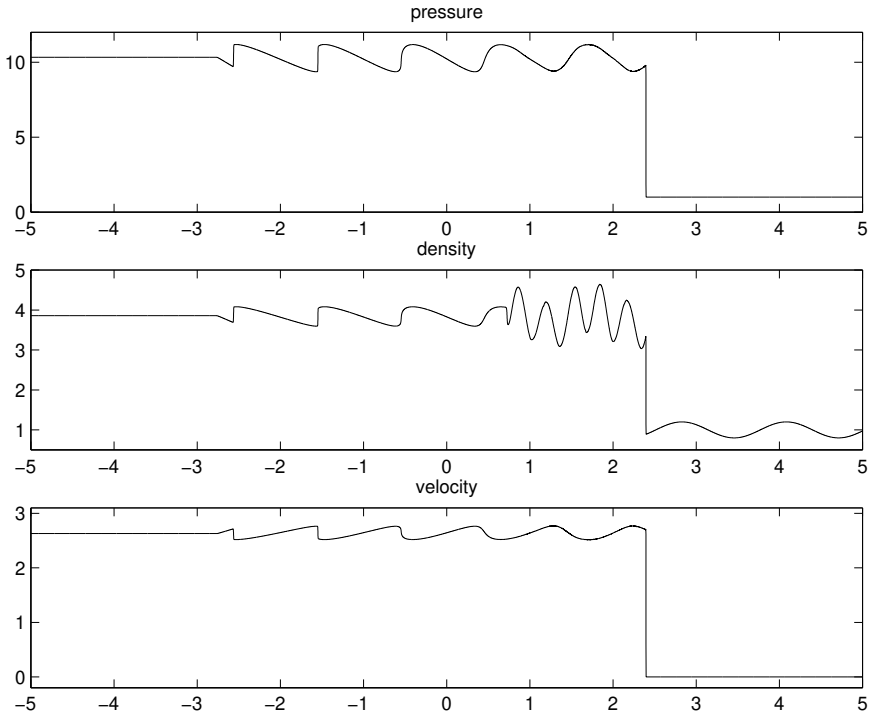

FIGURE 8. Reference solution of the vortex test case computed on a fine grid.

Figure 8 shows the solution at $t = 1.8$ computed on a fine grid over the domain $x \in [-5, 5]$.

In Figures 9 and 10 we show enlarged plots of the preshock and postshock region for three solutions computed using different limiting strategies: (i) the well-balanced van Leer limiter for all waves; (ii) the van Leer limiter for nonlinear waves and the $\mathrm{ACM}_{2.0}$ limiter for linear waves using a partial characteristic decomposition (PCD); and (iii) the compressive $\mathrm{ACM}_{2.0}$ limiter for all waves. The second strategy exhibits the stability observed for the van Leer scheme for the nonlinear waves (the three leftmost saw-tooth patterns) and at the same time captures the extremities of the complex linear-nonlinear wave pattern in the rightmost postshock region, which the van Leer computation was not able to resolve. In the preshock region, the PCD based scheme shows a slight tendency of sharpening the smooth sine waves but does not decrease the extreme values as the van Leer limiter does.

In [20] we have applied these techniques to the two-dimensional system of compressible gas dynamics. ACM enabled us to improve the resolution of contact waves and small vortices dramatically, but it did also create spurious oscillations when too much compression was added.

6. Discussion

To conclude this note, we would like to stress once more the power, but at the same time the danger of compressive limiters. These limiters are not only dangerous when applied to nonlinear fields, where they may compress rarefaction waves into entropy-violating shocks. They are already dangerous for linear advection equations: as soon as a step is resolved sharply within a few computational cells, kinks or even jumps should be expected in smooth parts of the solution.

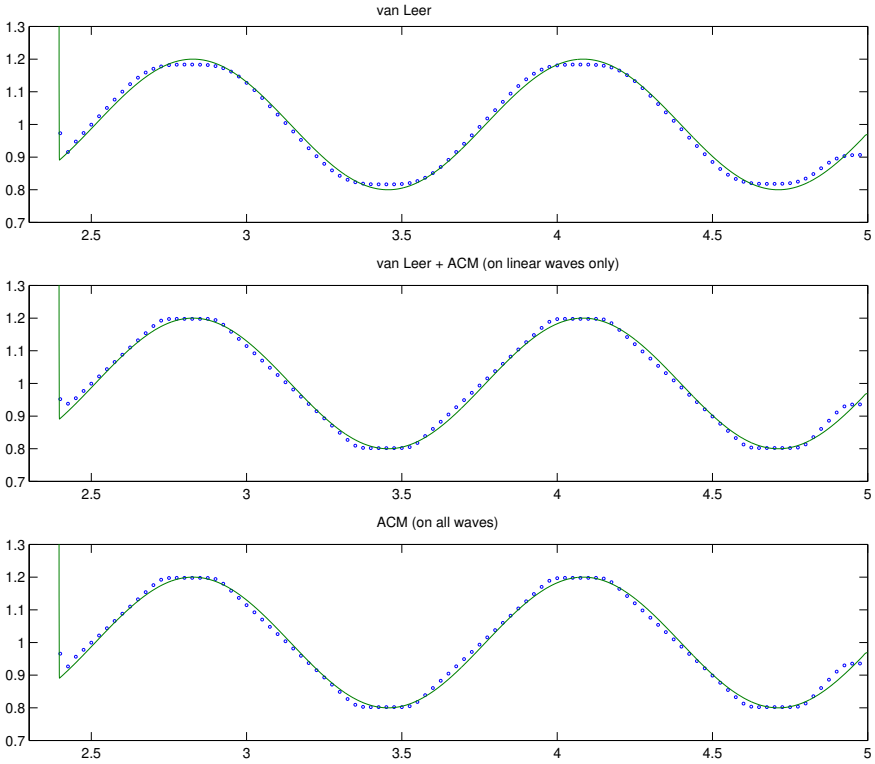

FIGURE 9. Comparison of solutions computed by three different limiting strategies, zoom on the preshock zone.

At the heart of the problem is Harten's switch function θ_i given in (20). As we have discussed in Remark 3, it cannot distinguish between corners of a step function and smooth extrema. We did experiment with other switch functions from [16, 21], but the tuning of parameters proved to be rather delicate.

We believe that it would be extremely desirable to design a more reliable switch function, which would make it possible to exploit the powers of the ACM method to its full extent.

REFERENCES

[1] S. K. Godunov. A finite difference method for the computation of discontinuous solutions of the equations of fluid dynamics. *Mat. Sb.*, 47:357–393, 1959.

[2] B. van Leer. Towards the ultimate conservative difference scheme V. A second order sequel to Godunov's method. *J. Comput. Phys.*, 32:101–136, 1979.

[3] P. Lax. Weak solutions of nonlinear hyperbolic equations and their numerical computation. *Comm. Pure Appl. Math.*, 7:159–193, 1999.

[4] H. Nessyahu and E. Tadmor. Non-oscillatory central differencing for hyperbolic conservation laws. *J. Comput. Phys.* 87:408–463, 1990.

[5] X.-D. Liu and E. Tadmor. Third order nonoscillatory central scheme for hyperbolic conservation laws. *Numer. Math.* 79:397–425, 1999.

[6] D. Levy, G. Puppo, G. Russo. Compact central WENO schemes for multidimensional conservation laws. *SIAM J. Sci. Comp.*, 22:656–672, 2000.

[7] P. Arminjon, D. Stanescu and M.-C. Viallon. A two-dimensional finite volume extension of the Lax–Friedrichs and Nessyahu–Tadmor schemes for compressible flows. *Proc. 6th. Int. Symp. on CFD, Lake Tahoe* M. Hafez and K. Oshima (eds.) , Vol. IV, pp. 7–14, 1995.

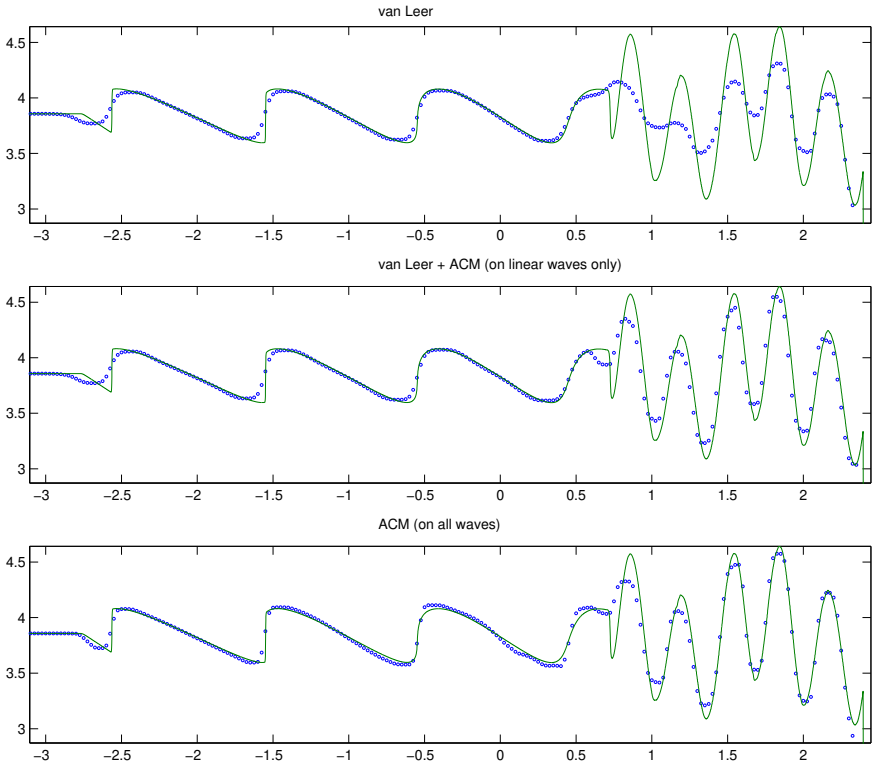

FIGURE 10. Comparison of solutions computed by three different limiting strategies, zoom on the postshock zone.

[8] G.-S. Jiang and E. Tadmor. Nonoscillatory central schemes for multidimensional hyperbolic conservation laws. *SIAM J. Sci. Comput.*, 19(6):1892–1917 (electronic), 1998.
[9] P. Arminjon, M.-C. Viallon and A. Madrane. A finite volume extension of the Lax–Friedrichs and Nessyahu–Tadmor schemes for conservation laws on unstructured grids. *Int. J. Comput. Fluid Dyn.* 9(1):1–22, 1997.
[10] P. Arminjon and M.-C. Viallon. Convergence of a finite volume extension of the Nessyahu–Tadmor scheme on unstructured grids for a two-dimensional linear hyperbolic equation. *SIAM J. Numer. Anal.* 36(3):738–771, 1999.
[11] A. Kurganov and E. Tadmor. New high-resolution central schemes for nonlinear conservation laws and convection–diffusion equations. *J. Comp. Phys.*, 160:214–282, 2000.
[12] A. Kurganov, S. Noelle and G. Petrova. Semi-discrete central-upwind schemes for hyperbolic conservation laws and Hamilton-Jacobi equations. *SIAM J. Sci. Comp.* (in print).
[13] S. F. Liotta, V. Romano and G. Russo. Central schemes for balance laws of relaxation type. *SIAM J. Numer. Anal.* 38:1337–1356, 2000.
[14] V. Romano and G. Russo. Numerical solution for hydrodynamical models of semiconductors. *Math. Models Meth. Appl. Sc.* 10:1099–1120, 2000.
[15] Y. C. Tai, S. Noelle, N. Gray and K. Hutter. Shock capturing and front tracking methods for granular avalanches. *J. Comput. Phys* (accepted for publication).
[16] A. Harten. High resolution schemes for hyperbolic conservation laws. *J. Comput. Phys.*, 49:357–393, 1983.
[17] P. Roe. Approximate Riemann solvers, parameter vectors, and difference schemes. *J. Comput. Phys.*, 43:357–372, 1981.
[18] A. Kurganov and G. Petrova. Central schemes and contact discontinuities. *M2AN* (submitted).
[19] P. K. Sweby. High resolution schemes using flux limiters for hyperbolic conservation laws. *SIAM J. Numer. Anal.*, 21:995–1011, 1984.

[20] K.-A. Lie and S. Noelle. High resolution nonoscillatory central difference schemes for the 2D Euler equations via artificial compression. Proceedings of the 11th ECMI Conference, Altavilla Milicia (Palermo), Italy, September 26-30, 2000 (in print).
[21] A. Harten. The artificial compression method for computation of shocks and contact discontinuities. III. Self-adjusting hybrid schemes. *Math. Comp.*, 32(142):363–389, 1978.

(Knut–Andreas Lie)
SINTEF Applied Mathematics,
P.0. Box 124 Blindern, N–0314 Oslo, Norway
Also: Department of Informatics, University of Oslo
E-mail address: Knut-Andreas.Lie@math.sintef.no
URL: http://www.ifi.uio.no/~kalie/

(Sebastian Noelle)
Institut für Geometrie und Praktische Mathematik,
RWTH Aachen, 52056 Aachen, Germany
E-mail address: noelle@igpm.rwth-aachen.de
URL: http://www.igpm.rwth-aachen.de/~noelle/